Chapter 2. Semiconductor Surface Studies

Academic and Research Staff

Professor John D. Joannopoulos, Dr. Kyeongjae Cho, Dr. Pierre Villeneuve

Graduate Students

Rodrigo B. Capaz, Shanhui Fan, Ickjin Park

Technical and Support Staff

Margaret O'Meara

2.1 Introduction

Sponsor

Joint Services Electronics Program
Grant DAAH04-95-1-0038

Understanding the properties of surfaces of solids and the interactions of atoms and molecules with surfaces is extremely important both from the technological and academic points of view. The advent of ultrahigh vacuum technology has made microscopic studies of well-characterized surface systems possible. The way atoms move to reduce the energy of the surface, the number of layers of atoms involved in this reduction, the electronic and vibrational states that result from this movement, and the final symmetry of the surface layer are all of utmost importance in arriving at a fundamental and microscopic understanding of the nature of clean surfaces, chemisorption processes, and the initial stages of interface formation.

The theoretical problems associated with these systems are quite complex. However, we are currently at the forefront of solving the properties of real surface systems. In particular, we are continuing our efforts to develop new techniques for calculating the total ground-state energy of a surface system from "first principles," so that we can provide accurate theoretical predictions of surface geometries and behavior. Our efforts in this program have concentrated on the areas of surface growth, surface reconstruction geometries, structural phase transitions, and chemisorption.

2.2 Mechanical Hysteresis on an Atomic Scale

Hysteresis is generally associated with two (or more) different pathways connecting two macroscopic equilibrium states. A classic example is a ferromagnetic system of spins in a uniform external magnetic field, where one can cycle repeatedly between two equilibrium points by varying the magnetic field. This is a macroscopic collective phenomenon. One can also envision a *microscopic* hysteresis phenomenon if it were possible to construct a *local* magnetic field that couples to only one spin of the system. Since a microscopic hysteresis involves a single spin, even a pure antiferromagnet, which exhibits no macroscopic hysteresis, could exhibit a microscopic hysteresis.

However, it has not been proved possible to generate a magnetic field which couples to only one spin of the system, and consequently this novel phenomenon of microscopic hysteresis has not been observed. There are, on the other hand, systems which are not magnetic but nevertheless belong to the same universality class as magnetic systems for which observation of a microscopic hysteresis may be possible. One particularly interesting example is the (100) surface of silicon which can be mapped onto a two-dimensional antiferromagnetic spin system. Such a mapping has been used to study the phase transition of the Si (100) surface in which each asymmetric surface dimer is associated with a single spin degree of freedom. What is interesting about this system is that if one were now to bring a sharp tip near the surface, as in atomic force microscopy, the force field between the tip and surface dimers would act like a local external magnetic field for the corresponding magnetic system.

To investigate the possible existence of a microscopic hysteresis effect in Si (100), we performed ab initio total energy calculations which describe the surface system in the presence of a tungsten tip

typically used in AFM experiments. The coupling strength and sign of the force between the AFM tip and a surface dimer is controlled by moving the tip up and down. The response of the dimer to the change of the external field is monitored by studying the changes in geometric structure and energy of the dimer configuration as a function of the tip height.

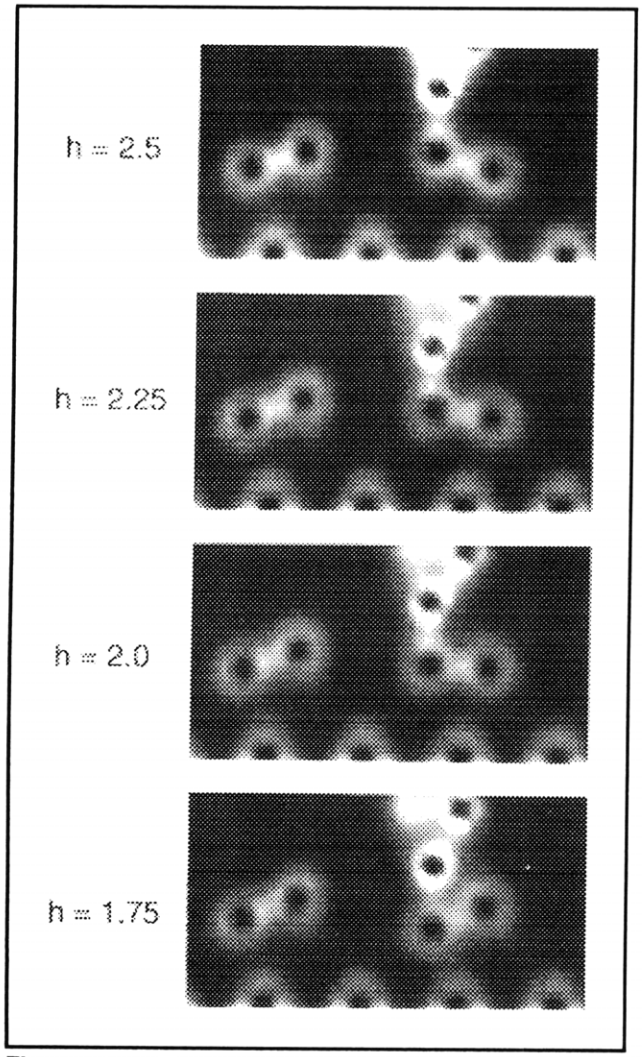

Figure 1. The sequence of charge density cross sections (from bottom to top) as the tip pushes down and flips the dimer. h is the tip-surface distance in Å defined as the distance of the top apex atom and the upper dimer atom before relaxation.

The four panels in figure 1 correspond to the sequence of decreasing the tip-surface distances, 2.5, 2.25, 2.0, and 1.75 Å. This sequence shows that as the AFM tip moves down, it *pushes down and flips* the surface dimer. The first three panels show a gradual decrease of the dimer angle (17°, 12°, and 2°), but the change of the equilibrium dimer-angle between the third panel and the fourth panel appears *discontinuous* (from 2° to – 24°).

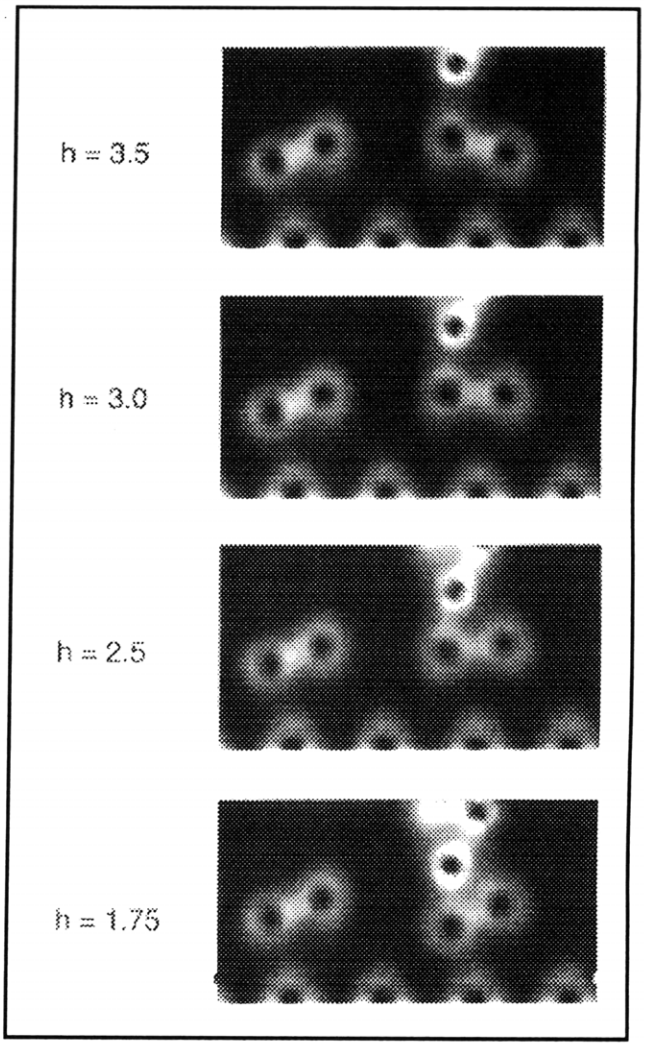

Figure 2. The sequence of charge density cross sections (from top to bottom) as the tip pulls up and flips the dimer. Same convention for h as in figure 1.

However, as the AFM tip moves up, the dimer configuration changes continuously as shown in figure 2. From the sequence of bottom to top, the tip-surface distance increases from 1.75 to 2.5 Å to 3.0 to 3.5 Å, and the dimer-angle increases gradually. This different behavior of dimer geometry clearly indicates that the dimer configuration follows two different local minimum energy paths as the tip moves down and up. The continuous up-path corresponds to a continuous transition in the Landau theory as illustrated in the right-hand sequence of figure 2. Therefore, the dimer configuration shows not only a quantitative difference but also a qualitative difference in the down-up cycle.

In order to make direct contact with AFM experiments for this system, we have calculated the force

on the tip for the two different pathways corresponding to lowering and raising the tip. The results are shown in figure 3. We note that the force-distance hysteresis loop exhibits a rather complex behavior. As the tip approaches the surface between 5.0 and 3.5 Å along the down-path, the force on the tip becomes more attractive and reaches a maximum at 3.5 Å. This corresponds to an inflection point in the interaction energy curve between the tip and surface. From 3.5 to 2.25 Å, one approaches a metastable equilbrium geometry for "adsorption" of the tip on the surface. At 2.25 Å the force is zero and the interaction energy is at its minimum. As the tip approaches closer to the surface, the force now becomes repulsive and at a distance of slightly less than 2 Å the dimer has flipped with a discontinuous change in its equilibrium angle. This corresponds to a process of overcoming a kink in the interaction energy. At this point the force is large and attractive since the tip would prefer to get closer to the down-dimer atom. This corresponds ultimately to the global adsorption energy minimum geometry.

As we now raise the tip from a distance of 1.75 to 3 Å, the force initially becomes slightly less attractive up to 2.5 Å and then reverts to becoming slightly more attractive from 2.5 to 3 Å. This corresponds directly to the tip atom being allowed to relax more during the first phase (1.75 → 2.5 Å). At 3 Å, the dimer angle has just changed sign. As the tip-surface distance increases further, the dimer gradually reverts to its original flipped geometry, and the force on the tip approaches zero.

This investigation leads to the prediction that the Si(100) surface in the presence of a tungsten AFM tip does indeed provide a potentially observable example of mechanical hysteresis on a microscopic or atomic scale.

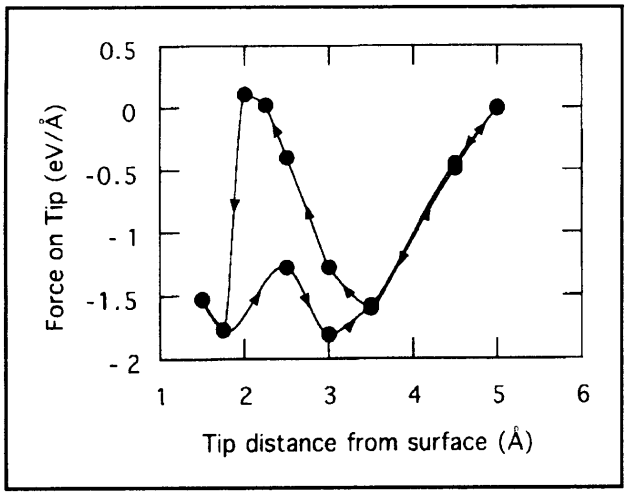

Figure 3. The hysteresis loop of the force on the AFM tip as the tip moves down (left arrows) and up (right arrows).

2.3 Heteroepitaxial Growth

Understanding epitaxial growth is a long-standing unsolved problem in condensed matter physics. An atomistic, theoretical approach is extremely difficult because the many different physical processes, such as adsorption, diffusion, re-evaporation, are complex and occur simultaneously at high temperatures. Computer simulations such as Monte-Carlo or molecular-dynamics are the obvious way to describe these phenomena. However, large-scale simulations can only be done for a restricted class of materials that can be accurately described by empirical or semi-empirical interatomic potentials.

One very important technological system involving heteroepitaxial growth is GaN on (0001) 6H-SiC, and for this system an ab initio treatment is required. In this work we have applied our ab initio techniques to investigate the nature of the initial stages of heteroepitaxial growth in this system. Since both SiC and GaN are partly ionic and partly covalent bonded materials with different degrees of ionicity and bond strengths, it is not obvious which bonding configuration will prevail at the interface. Although fundamental for the understanding of the growth process in these materials, very little attention has been given in the literature to the issue of GaN polarity on SiC substrates. Thus, total energies of four different types of interfaces were calculated, corresponding to Si-terminated or C-terminated substrates and Ga-terminated or N-terminated epilayers.

Contour plots of the total valence charge density and schematic ball-and-stick models for the four types of interfaces are displayed in figure 4. The plane of cut for all the figures is the hexagonal $(10\bar{1}0)$ plane, which contains two of the four bonds of the tetrahedrally coordinated atoms. The ball-and-stick models superimposed on each charge density plot give faithful description of the bond lengths and bond angles for each structure. Notice that the C and N atoms are surrounded by regions of high density of contours, reflecting the displacement in the bond maximum density towards these two atoms with higher electronegativity. Accordingly, Si and Ga atoms correspond to regions of depletion of valence charge density and "look smaller" compared to C and N. Let us denote by E_a, E_b, E_c and E_d the total energies of the four interfaces displayed in figures 4a, 4b, 4c and 4d, respectively. Figure 4a corresponds to a Si-terminated substrate and ideally Ga-terminated film. Notice that the Si and N atoms at the interface form

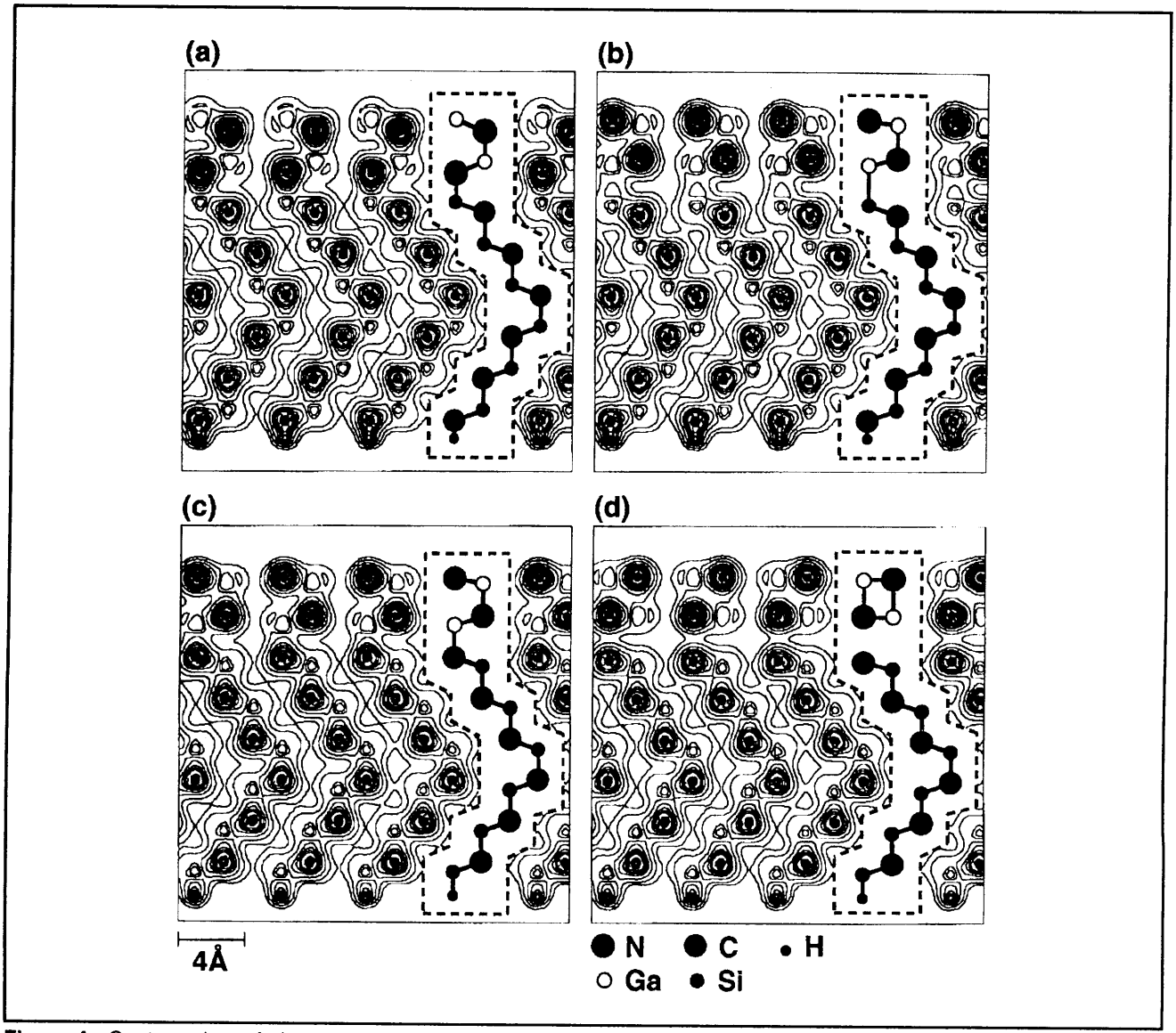

Figure 4. Contour plots of electronic density for four interfaces. Twelve evenly spaced contours from 0.4 to 3.7 (in units of electrons/Å^3) are used. Two additional contours at 0.1 and 0.2 help to map the low charge density regions. Ball-and-stick models are superimposed for each case. Balls are placed at the actual atomic positions and differ by shade and size according to the atomic types.

a partly covalent, partly ionic bond. The Si-N bond distance is 1.77 Å. The remaining bond lengths and angles do not change significantly from the bulk values and the initial epilayers of the film look like a smooth continuation of the substrate. Figure 4b still corresponds to a Si-terminated substrate, but the film is now ideally N-terminated. A covalent bond is formed between Si and Ga at the interface (the bond distance is 2.43 Å). However, this bond is very weak since most of the charge remains concentrated around the C and N atoms. Subtraction of E_b from E_a gives us $E_a - E_b = -1.08$eV, indicating that for Si-terminated substrates, the ideally Ga-terminated film with Si-N bonds at the interface is energetically favorable.

A similar situation occurs for C-terminated substrates (figures 4c and 4d). In figure 4c, the ideally N-terminated film with C-Ga bonds at the interface is shown, and the charge density contours resemble very much those of figure 4a with inverted polarity. A strong covalent and ionic bond between C and Ga (bond length 1.99 Å) is formed at the interface. However, for ideally Ga-terminated films (figure 4d) the situation is surprisingly distinct from all the previous cases. The N atoms at the interface prefer to make bonds along the c-axis to the nearby Ga atoms (bond distance 2.22 Å) than to the C atoms on the substrate, yielding a very weakly coupled film-substrate system. The angles

between all the Ga-N bonds shown in the figure are very close to 90°, indicating sp^2 hybridization of the epilayers. Although carbon and nitrogen form strong covalent bonds in a large variety of situations, the presence of the surrounding atoms seems to make polarization effects very crucial, and the C and N atoms behave almost like two repelling negative charges. The total energy difference, $E_c - E_d = -1.07eV$, suggests that *for C-terminated substrates, the ideally N-terminated film with C-Ga bonds at the interface is energetically favorable.*

The results above suggest that the importance of the strength of covalent bonds is diminished by the polarization induced by the surrounding atoms and the ionic component of the bonds prevails. Thus our findings can be described in terms of a very simple rule of polarity matching at the surface. The lowest energy interfaces are those on which "positive" substrate ions bind to "negative" film ions, and vice-versa. Therefore the GaN films will grow with the same polarity as the SiC substrates. Besides being intuitively appealing, this picture is strongly supported by the fairly big energy differences (~1 eV per surface atom) we found in our calculations. We believe that it is also robust enough to describe other possible microscopic processes during the initial stages of growth (for example, replacement of substrate ions by film ions at the interface should also satisfy polarity matching).

2.4 Publications

Capaz, R., K. Cho, and J.D. Joannopoulos. "Signatures of Bulk and Surface Arsenic Antisite Defects in GaAs(110)." *Phys. Rev. Lett.* 75: 1811 (1995).

Capaz, R., H. Lim, and J.D. Joannopoulos. "Ab initio Studies of GaN Epitaxial Growth on SiC." *Phys. Rev. B* 51: 17755 (1995).

Chen, J., H. Haus, J. Winn, S. Fan, and J.D. Joannopoulos. "Wide Stop Band Optical Filters from PBG Air Bridges." In *Guided-Wave Optoelectronics.* Eds. Tamir, Bertoni, and Greffel. New York: Springer Verlag, 1995.

Chen, J., H. Haus, S. Fan, and J.D. Joannopoulos. "Optical Filters from PBG Air-Bridges." Paper published in the *Proceedings of the European Conference on International Optics,* The Netherlands, 1995.

Cho, K., and J.D. Joannopoulos. "Tip-induced Modifications in Scanning Tunneling Microscopy and Atomic Force Microscopy." *Scan. Microscopy* 9: 381 (1995).

Cho, K., and J.D. Joannopoulos. "Mechanical Hysteresis on an Atomic Scale." *Surf. Sci.* 328: 320 (1995).

Fan, S., P. Villeneuve, and J.D. Joannopoulos. "Theoretical Investigation of Fabrication-Related Disorder on the Properties of Photonic Crystals." *J. Appl. Phys.* 78: 1415 (1995).

Fan, S., A. Devenyi, R. Meade, and J.D. Joannopoulos. "Guided Modes in Periodic Dielectic Materials." *J. Opt. Soc. Am. B* 12: 1267 (1995).

Joannopoulos, J.D. "An Introduction to Photonic Crystals." Paper published in the *Proceedings of NATO ASI,* Crete, 1995.

Joannopoulos, J.D. "The Almost-Magical World of Photonic Crystals." Paper published in the *Proceedings of the Seventh Brazilian Workshop on Semiconductor Physics,* Rio de Janeiro, Brazil, 1995.

Villeneuve, P.R., and J.D. Joannopoulos. "Tricks of the Light." *New Sci.* 147(1992): 26 (1995).

Villeneuve, P., S. Fan, J.D. Joannopoulos, K. Lim, G. Petrich, L. Kolodziejski, and R. Reif. "Air-Bridge Microcavities." *Appl. Phys. Lett.* 67: 167 (1995).

Villeneuve, P.R., S. Fan, I. Kurland, J.C. Chen, and J.D. Joannopoulos. "Photonic Bandgap Structures and Devices." *QELS Tech. Digest Series* 15 (1995).

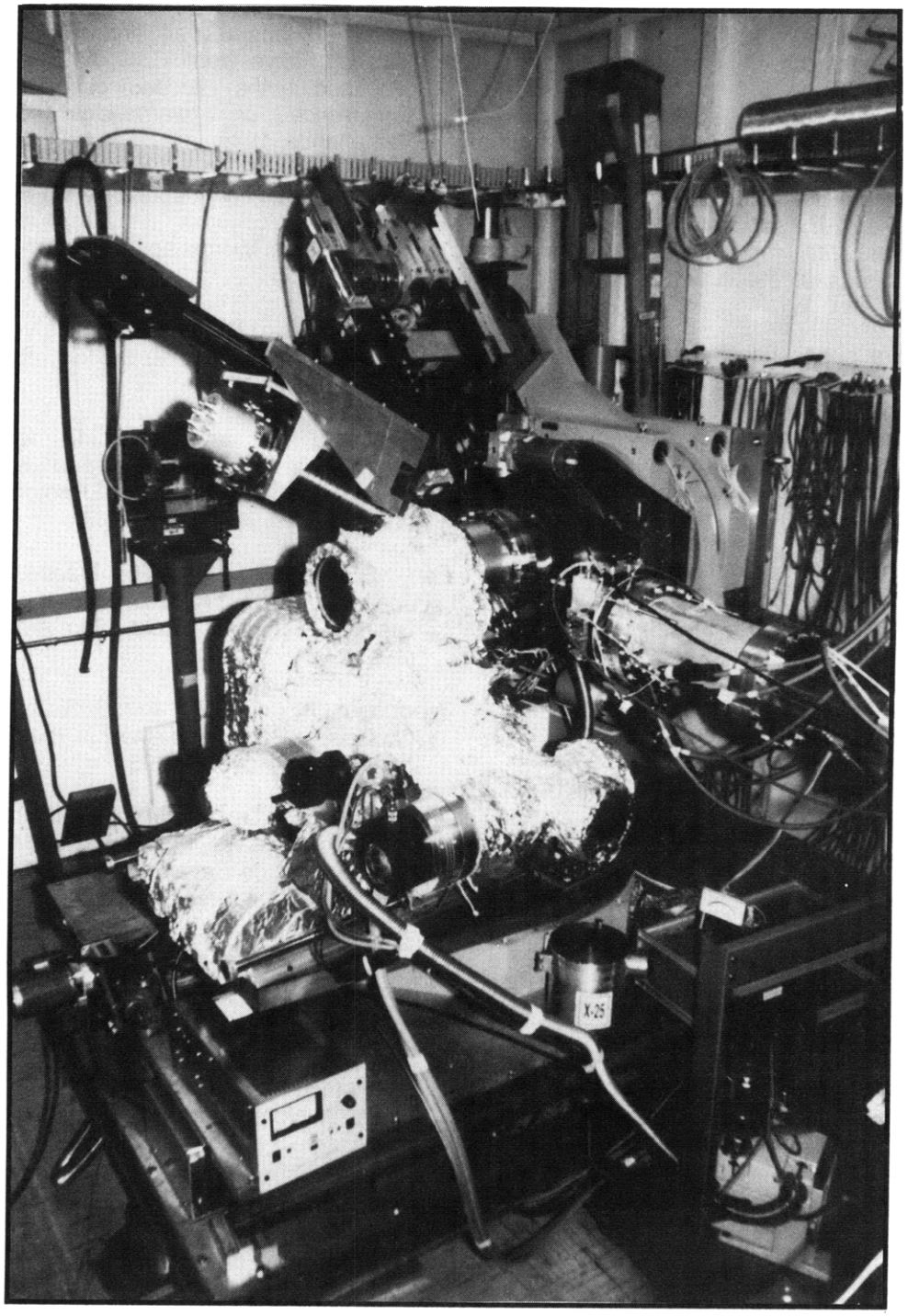

The MIT ultra-high vaccum apparatus for surface x-ray scattering in the hutch of the X25 beamline at the National Synchrotron Light source at Brookhaven National Laboratory.